Estimation of the characteristics of reflected radiation as applied to monostatic and bistatic laser sounding of crystal clouds containing oriented particles

O.V. Shefer

Tomsk State University

Received June 4, 2003

A comparative estimate is presented of the high-intensity radiation reflected from cloud crystals of different shape. Ensembles of ice plates are chosen in model investigation of crystal clouds containing oriented particles. The expressions obtained for scattering coefficients in the frameworks of physical optics make it possible to study angular distribution of the intensity of scattered radiation as well as its polarization properties. Also, the advantages of bistatic laser sounding over the monostatic one are mentioned. It is shown that one can determine the size spectrum of plates and the plate flatter in atmospheric formation of inhomogeneous composition from variations of absolute and relative values of the scattering coefficient obtained at near-forward scanning by moving the source. In addition, one can estimate the refractive index and orientation of particles in space from the data on polarization characteristics of scattered radiation.

Subject of the study

Physical properties of crystal clouds

Crystal clouds are extended over the greater part of the Earth surface. Their composition is presented by a tremendous variety of particle habits and size. One of the most complete classifications of the habits of water ice crystals contains more that 80 types.[1] According to the conditions of crystallographic growth (i.e., at certain values of pressure, temperature, electric field, etc.), one or another type of particles is prevalent in a cloud.[1–3] Clouds with small water content (as a rule, less then 0.05 g/m^3) at temperatures near −20°C mainly consist of plates. In particular, as is noted in Ref. 4 about 80% of crystal particles in cirrus clouds formed over mountains are ice plates. The elongated particles such as hexagonal columns, needles, and plates are observed in practically all mixed and crystal clouds.

Optical properties of atmospheric crystals are such that the mean statistical values of the refractive index ($\tilde{n} = n + i\chi$) show that they are similar to pure ice. However, airflow involves aerosol, which then settles on large particles. The contamination of ice crystals depends on their shape and size.[5] In particular, it is revealed that real part n of the refractive index in the visible wavelength range can vary from 1.35 to 1.75, and the imaginary part χ depends on the concentration of soot particles (χ of the background aerosol varies from 0–0.05, and χ of industrial aerosol is ≈ 0.1).

The particle motion in the calm atmosphere is caused by aerodynamic and gravity forces. Obviously, the crystals are oriented so that the normal to their maximum area coincides with the direction of motion and the air resistance is greatest. Plates are most stable in space among the elongated particles. They are subject to smallest oscillations relative to the predominant orientation plane.

The behavior of particles in the atmosphere depends on the motion of air masses. Re-orientation of each particle is determined by the difference in the vectors of the velocity of its fall and the wind velocity. The large-scale vortices, as a rule, cannot change the motion of the predominantly oriented ensemble of particles, as the velocity of such a flow is less than the velocity of the crystal fall.[6]

All force fields affect the regularities of the air mass circulation. The deep inhomogeneities of the Earth, breaks of geological structures, fluctuations of the magnetosphere, electric field – all this affects the atmospheric stratification.[7] As a rule, the presence of the force field favors the stable position of a particle in space. For example, the effect of electric field leads to the strong orientation of particles. However, the degree of this effect on the ensemble of crystals, as a whole, significantly depends on their shape and initial orientation.[6–9]

At present, great attention is paid in the world to the study of crystal clouds. The atmospheric optical phenomena caused by interaction of optical radiation with ice crystals[2,3] are of special interest of researchers. One can observe color circles in the atmosphere called corona,[10] because of the diffraction of light on small chaotically oriented crystals. Depending on the Sun position, refraction of light on hexagonal crystals leads to formation of a halo. Sun pillars are the result of reflection of sunlight from elongated oriented particles. In spite that the physical nature of these optical phenomena is known for a long time, the peculiarities of each of them are to be studied.

Lidar methods of sounding are widely used for the study of crystal clouds. As a rule, the cross-polarized component appears in the return signal at

0235-6880/03/09 729-11 $02.00

interaction of linearly polarized optical radiation with non-spherical particles. It is explained by the fact that the state of polarization of the incident radiation can change due to variations of microphysical, optical, and orientation properties of scatterers. In this connection, polarization lidars, along with non-polarization ones, provide for obtaining more data on the scattering media studied. High potential in the study of cirrus clouds can be realized at remote sensing by means of a bistatic polarization lidar. Researchers mention the advantages of this method over traditional monostatic sounding.[11]

Some peculiarities of the methods for calculation applied to the problems of scattering on polyhedrons

To date, the numerical models of particles with both chaotic and predominant orientation are available. Analysis of current methods for solving the wide range of scattering problems is presented in Refs. 12 and 13. By virtue of difficulties in numerical simulations of the process of scattering, especially by oriented crystals, different mathematical methods are applied, resulting from which the domain of applicability of the models becomes narrower. In this paper we consider only the peculiarities of the principal method, including the geometric optics approximation, in determining the scattering from large semi-transparent particles. This method enables us to follow the trajectory of any beam taking into account its multiple reflections inside a particle.

Ice particles, because their crystallographic structure, are well pronounced polyhedrons. Let the electromagnetic field be incident on the crystal. The field after interaction is a discrete set of beams of parallel rays. One or another direction of each beam is caused by division of the field at edges and tops of the crystal. Such a structure of the scattered field in the near zone excludes the possibility of using further the method of geometric optics. It is explained by the fact that, from the standpoint of this method, the zone around the scatterer, except for some directions, is the zone of the geometric shadow.

Situation for determination of the scattered field by chaotically oriented particles is different. The vectors of refracted beams outgoing from the crystals continuously fill the area of the total solid angle. In this case, one can assume that there are no "prohibited" zones for the refracted beams. Hence, the scattering characteristics of the crystal with chaotic orientation can be obtained by means of the geometric optics method.

The wave front after interaction with a polyhedron is plane. The "diffraction effect" is used for determination of the field in the wave zone.[1] Numerically that means application of δ-function with its restriction in infinity. In this case, one does not take into account the beam size in calculating the light scattering characteristics, but perform integration over the geometric shadow. There is also a different approach. The Fraunhofer integral[12] is used in the frameworks of the method of physical optics for recalculation of the fields from the near zone to the wave zone. The scattered field of each beam is δ-shaped, the same as the diffraction field of a large particle. The full scattering diagram is strongly indented and is characterized by sharp peaks of different magnitude along the directions of outgoing beams.

One should note that taking into account only the first maximum in calculating the Fraunhofer integral does not allow one to calculate the scattered field of the beam out of this zone. It is especially important for determination of scattering of large beams along the directions different than the directions of propagation (for example, in the case excluding the specular reflection from the plate bases).

One should note that one usually consider a non-absorbing particle in order to simplify the solution of the problem, though the cloud crystals are semi-transparent. Neglect of the imaginary part of the refractive index, even at visible wavelengths, cannot represent real situation.[14] It is more valid for particles where the beam (or ray) passes a long path multiply reflecting from the crystal sides.

The results of numerical simulation of the process of the electromagnetic field scattering on oriented crystals presented below were obtained in the frameworks of a hybrid method, which combines the methods of geometric and physical optics. The first of them enables one to determine the scattered field in near zone taking into account the wave nature of the incident radiation as a set of diverging beams of parallel rays outgoing from the crystal, and the second is used for recalculation of the field from near to the wave zone. This method for calculation is more effective for description of scattering of polarized optical radiation by a large oriented crystal in vector form.[15] The data on polyhedron shape of a semi-transparent crystal are introduced in it by means of a system of algorithms, and the fine structure of the field transformed by an anisotropic scatterer is determined.

Estimation of the radiation intensity reflected from cloud crystals

It is known that an atmospheric formation at negative temperature consists of ice crystals different in shape and size, not excluding the liquid-droplet phase. Let us divide all particles into three groups according to the peculiarities of scattering. Let the first group contain the volume shaped particles. As a rule, they are chaotically oriented in space. Small plates and columns without any certain position in space also can be related to this group. Let the second and third groups contain predominantly oriented crystals of plate and column shape. Obviously, the volume crystals isotropically scatter the radiation. The increase of the radius of curvature

of the reflecting surface causes a prevalent direction of reflection. In testing ice clouds, researchers have observed bright light fluxes reflected from the crystals. In analyzing the data of laser sounding, one should take into account the contribution of each type of crystals into the intensity of return signals. The vast material illustrating the results of sounding of atmospheric formations containing oriented crystals can be found in the literature.[1,13] In experimentally studying crystal clouds, researchers estimated the dependence of the backscattering coefficient on the ratio of the number densities of isotropically scattering particles and oriented crystals of an extended shape taking into account their flatter. It is shown that even small number of oriented crystals (several percent) leads to sharp (about several orders of magnitude) increase in the amplitude of the return signal.[16,17]

Let us consider the scattering by a hexagonal column.[15] To do this, let us determine the value $g_1 = \sigma_{sc}^1 / s$, where σ_{sc}^1 is the scattering cross section, to which the intensity of the scattered field is proportional, s is the area of the geometric shadow in the wave front after interaction of radiation with the particle. Let the wave with circular polarization is incident on a right prism, and the plane of incidence be perpendicular simultaneously to the base and one of the sides. Let the angle between the direction of the wave propagation and the side be 30°. The scattering diagram taking into account up to three multiplicities of reflection of the refracted beams in the crystal is shown in Fig. 1.

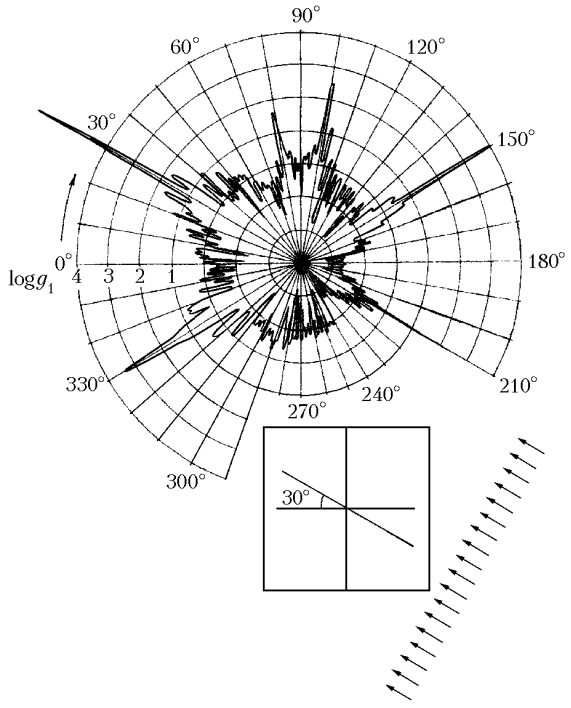

Fig. 1. Scattering diagram of the wave in the plane of its incidence taking into account up to triple passing of the refracted beams through a hexagonal crystal. Incidence plane of the wave is perpendicular to the side and to the crystal base.

Input parameters are the following: the wavelength $\lambda = 0.55$ μm, the length of the edge of the prism base $a = 60$ μm, the length of the side edge $l = 300$ μm, the refractive index of the crystal $\tilde{n} = 1.31 + i10^{-4}$. It is seen in Fig. 1 that the maxima are δ-shaped, but their amplitudes are finite. Each of the maxima of the diagram is caused by one or another cross section of the beam outgoing from the crystal either after interaction of radiation with the crystal surface or after two or three reflections. The beams are formed at division of the field at the edges and tops of the hexagonal crystal. Let us note that the diagram region from 90 to 270° illustrates scattering into the backward hemisphere, and the diagram lobe at 210° shows the intensity of backscattering (along the counter direction relative to the direction of incident wave).

The scattering diagram in the plane parallel to the base of the crystal in the case of normal incidence of the wave on the side is shown in Fig. 2.

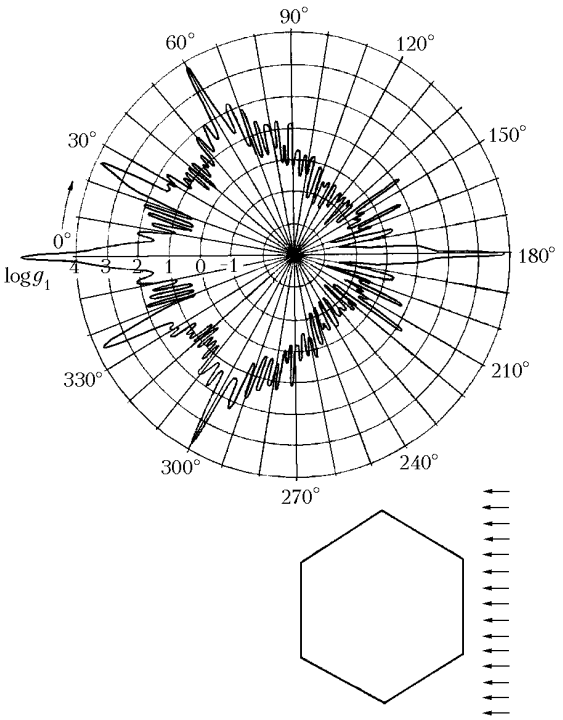

Fig. 2. Scattering diagram of the wave at its normal incidence on the side taking into account up to triple passing of refracted beams through a hexagonal crystal. $\lambda = 0.55$ μm, $\tilde{n} = 1.31 + i10^{-4}$, $a = 60$ μm, $l = 300$ μm.

Overwhelming part of the electromagnetic energy is scattered by a polyhedron in the direction of the refracted beams going out of it. The greater beam axes lie in one or another scattering plane, the more energy is scattered in this plane, the more is the area of the scattering diagram. The diffraction field together with the scattered field of the beams going out after multiple reflections determines the maximum lobe along the direction near 0° angle. Other maxima of the scattering diagram provide for

the refracted beams which go out of the crystal after one or several passes through it.

Thus, we have considered the examples of the scattering diagrams at possible extreme positions of the side relative the incident radiation for the case of a hexagonal column horizontally oriented in space. Rectangular sides of the crystal can be situated arbitrarily relative to the direction of incidence. In calculating the characteristics of reflection for the ensemble of columns, one should average the corresponding values characteristic of a single column over orientations. Obviously, the peculiarities of scattering will be smoothed. One should expect the return signal of higher amplitude in the case of reflection from the bases.

Let us carry out comparative analysis of the cross section ratios for three selected groups of particles, namely, crystals of volume shape, columns, and plates. Let us use the Mie solution for determining the reflection from isotropically scattering particles, and the models calculated in the frameworks of physical optics for columns and plates.[15,18]

The values of the ratio of the backscattering cross sections $\sigma_\pi^{pl}/\sigma_\pi^{cl}$ (curves *1* and *3*) and $\sigma_\pi^{pl}/\sigma_\pi^{sp}$ (curves *2* and *4*) are shown in Fig. 3. The backscattering cross sections σ_π^{pl} and σ_π^{cl} are obtained at the normal incidence of radiation on the plate base and the greatest symmetry axis of a rectangular prism, respectively.

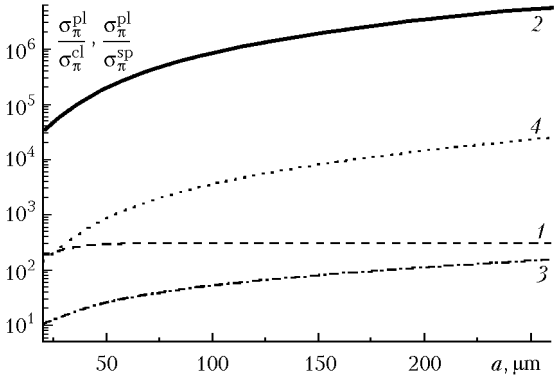

Fig. 3. Cross section ratios as functions of the particle size $\tilde{n} = 1.31 + i\cdot10^{-3}$; $\sigma_\pi^{pl}/\sigma_\pi^{cl}$, $\lambda = 0.694$ μm (*1*), $\sigma_\pi^{pl}/\sigma_\pi^{sp}$, $\lambda = 0.694$ μm (*2*); $\sigma_\pi^{pl}/\sigma_\pi^{cl}$, $\lambda = 10.6$ μm (*3*), $\sigma_\pi^{pl}/\sigma_\pi^{sp}$, $\lambda = 10.6$ μm (*4*).

Averaging over orientations caused by rotation about the maximum axis was performed for a hexagonal column. Curves *2* and *4* in Fig. 3 illustrate, how many times the backscattering cross section of a plate exceeds the corresponding value of a sphere σ_π^{sp}. Calculations of the characteristics were carried out for the crystals of comparable sizes. The plate radius was equal to the sphere radius, and the plate base area was equal to the prism side area. It is seen in Fig. 3 that the difference between the scattering characteristics reaches several orders of magnitude. The shorter is the wavelength of the incident radiation and the greater is the particle size, the more significant is the difference in the relevant quantities of reflected radiation.

One should note that the same conditions of particle growth cause the same mean size. Actually, the side areas of the column are 2–3 times less than the plate base area. Besides, it is known that possible oscillations of columns about the plane of their preferred orientation in the atmosphere exceed the plate flatter by several degrees.[19] All this leads to a decrease in the intensity of radiation reflected from columns as compared with that from plates, at least, by 1–2 orders of magnitude. Thus, when testing a cloud of complex composition containing oriented crystals, the plate-shaped crystals provide for the most intense reflection.

Numerous experimental investigations show that natural water ice clouds consist of particles exhibiting a great variety of shapes, size, and orientation. These physical properties of particles determine one or another pattern of scattering of radiation along with its polarization properties. In analyzing the sounding data on the mean values of such atmospheric formations, one can obtain only qualitative estimates of the medium. However, in studying well-pronounced peculiarities of scattering caused by some types of crystals (among which there are plates, in particular) one can obtain quantitative estimates of the formation under study. One should note that certain geometric parameters of plates, their number density and orientation are related to quite specific physical conditions in the atmosphere, which, at the same time, determine the structure of a cloud as a whole.[1,20] Let us consider a system of oriented plates as a crystal cloud. The basis for such a choice is given in our earlier paper.[18]

The optical methods are widely used now for the study of crystal clouds, against which the bistatic laser sounding stands out.[11] Information content of the ratio of the backscattering coefficients, one of them was obtained at the vertical position of the lidar, and another was obtained at its small deviation from the vertical direction, was studied for the ensemble of horizontally oriented ice plates.[21] The possibility of estimating the plate size and flatter from the data of monostatic laser sounding is also shown in this paper.

However, the difficulties can appear in the interpretation of data on "anomalous" backscattering, because of the absence of *a priori* data. In particular, the deficiency of additional data on the composition of cloud and orientation of particles does not allow one to correctly isolate the values of intensity caused by specular reflection from plates from the data of monostatic sounding. One should take into account that the high-amplitude return signal can be formed at reflection from large-size (hundreds or thousands of micrometers) spherical particles or plane sides of hexagonal columns. Besides, the state of polarization of the incident radiation is not changed both at specular reflection from plates and at reflection from

spherical particles. However, all difficulties of analysis of the data related to the aforementioned uncertainty in the case of monostatic sounding are eliminated at passing to the bistatic optical arrangement of sounding.

In sounding crystal clouds using such a lidar, one can fix the maximum possible intensity of the mirror-reflected signal on the receiving device along with the specific polarization characteristics related to a certain type of particles. This makes it possible to exclude ambiguity in analyzing the data of sounding atmospheric formations of a complicated structure. Moreover, the advantage of a bistatic sounding over the monostatic one lies also in the fact that it allows one to combine two contradictory requirements, if the lidar transmitter and receiver are joined. On the one hand, the necessity appears at monostatic sounding of recording the signal with "anomalously" high amplitude for estimating the parameters of a crystal clouds. On the other hand, one should take into account that the polarization characteristics (in particular, depolarization ratio) bear more information for determination of the crystal orientation and their refractive index, the stronger the lidar axis deviates from the vertical direction, and, hence, the weaker is the backscattering signal.[22] The high-amplitude polarized signal containing the complete information about optical, orientation, and microphysical properties of the tested crystal cloud can be obtained with the receiver of a bistatic polarization lidar even at specular reflection of sounding radiation.

It should be noted that though the bistatic lidars have been used since long ago no satisfactory theoretical investigations applicable to interpretation of the data of sounding of crystal clouds have been developed so far. One mainly use theoretical results applied to the monostatic laser sounding. The numerical model of a dispersed medium is presented in this paper in the form of a system of oriented plate-shaped crystals as applied to both bistatic and monostatic sounding optical arrangements.

Positions of source, receiver, and scatterer in a bistatic optical arrangement of sounding

Let us present the angular diagram of the positions of the sounding radiation source, receiver, and scatterer as applied to the bistatic sounding (Fig. 4). Let the radiation source be at the point O_1, the receiver at the point O_2, and the object under study at the point O_3. Let us set the absolute coordinate system $Oxyz$, in which three additional coordinate systems $O_1x_1y_1z_1$, $O_2x_2y_2z_2$, and $O_3x_3y_3z_3$, are introduced being related to the sounding radiation source, receiver, and a scatterer, respectively. The coordinate plane Oxy is parallel to the ground surface, and the normal direction to it lies along the axis Oz. The wave vector $\mathbf{k}$ indicates the direction of propagation of the incident radiation ($\mathbf{k} \parallel O_1z_1$). Electric components of the incident wave of elliptic polarization ($\mathbf{E}_1$, $\mathbf{E}_2$) oscillate along the O_1x_1 and O_1y_1 axes, respectively. The system of plates having same orientation was selected as a scatterer. Let us call the plane parallel to the plate bases the plane of preferred orientation. Let us denote this plane as $O_3x_3y_3$ and let us accept it as the coordinate plane; β is the angle between the direction of sounding $\mathbf{k}$ (or axis O_1z_1) and normal direction to the plate base $\mathbf{n}$ (or axis O_3z_3). The beams underwent specular reflection from the plate base or going out after a number of internal reflections are formed along the direction $\mathbf{k}_{\text{ref}}$ ($\mathbf{k}_{\text{ref}} \parallel O_3z_{\text{ref}}$). The elevation angle ψ and the azimuth angle ξ determine possible oscillations of the plate about the O_3z_3 axis. When changing ξ from 0 to 2π and the set value $\psi' = \psi$, the line normal to the plate base circumscribes a cone with the axis O_3z_3. Receiving of the scattered radiation is performed along the direction $\mathbf{k}_{\text{sc}}$ (or along the O_2z_2 axis), and the axis O_2z_2 is parallel to the horizontal plane (or the ground plane). The quantities $\mathbf{E}_{\text{I}}$ and $\mathbf{E}_{\text{II}}$ are the components of the field recorded with a detector. They are directed along the O_2x_2 and O_2y_2 axes, respectively. Let us denote by ϑ the deviation of the direction of receiving from the line of "strong" specular reflection (i.e., the angle between the directions O_3z_{ref} and $\mathbf{k}_{\text{sc}}$). The vector $\mathbf{k}_{\text{sc}}$ can be directed toward any point of the back hemisphere. The back hemisphere is referred to the part of the sphere limited by the plate base and containing the incident and reflected beams. In this connection, π is introduced as an index in notations of the light scattering characteristics presented below. Let us note that in the case of monostatic sounding $\mathbf{k} \parallel \mathbf{k}_{\text{sc}}$.

To present the normalized light scattering characteristics, it is enough to determine the angular position of unit vectors that set the components of the scattered field. In this connection, let us join the centers of all four coordinate systems at the point O and determine the angular dependences of the basis vectors ($\mathbf{x}$, $\mathbf{y}$, $\mathbf{z}$) of the absolute coordinate system with the basis vectors ($\mathbf{x}_i$,$\mathbf{y}_i$,$\mathbf{z}_i$) by the following relationship:

$$\begin{pmatrix} \mathbf{x} \\ \mathbf{y} \\ \mathbf{z} \end{pmatrix} = S_i \begin{pmatrix} \mathbf{x}_i \\ \mathbf{y}_i \\ \mathbf{z}_i \end{pmatrix}, \; i = 1, 2, 3,$$

where

$$S_i = \begin{pmatrix} \cos\varphi_i \cos\vartheta_i & -\sin\varphi_i & \cos\varphi_i \sin\vartheta_i \\ \sin\varphi_i \cos\vartheta_i & \cos\varphi_i & \sin\varphi_i \sin\vartheta_i \\ -\sin\vartheta_i & 0 & \cos\vartheta_i \end{pmatrix}.$$

Obviously, the angles ϑ_i, φ_i determine the position of the basis vectors $\mathbf{x}_i$,$\mathbf{y}_i$,$\mathbf{z}_i$ ($i = 1, 2, 3$) of each coordinate system $Ox_iy_iz_i$ ($i = 1, 2, 3$) with respect to the absolute system $Oxyz$.

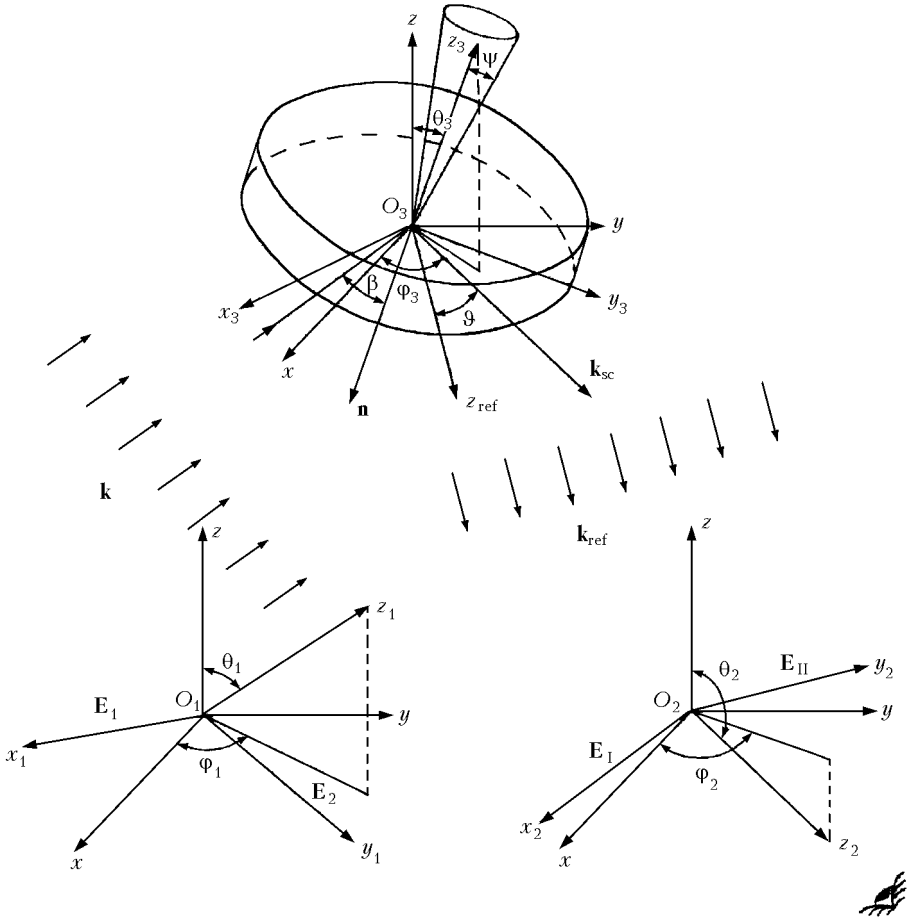

Fig. 4. Bistatic laser sounding diagram.

Characteristics of the specular return for the case of oriented plates

Let some quantity of the plate-shaped crystals be set *a priory*. Let us describe the particle size spectrum by the gamma-distribution[1]

$$N(a) = N\ \frac{\mu^{\mu+1}}{G(\mu+1)}\ \frac{1}{a_m}\ \left(\frac{a}{a_m}\right)^{\mu} \exp(-\mu a/a_m), \quad (1)$$

where N is the plate number density, a_m is the plate radius corresponding to the maximum of the function $N(a)$, μ is the dimensionless parameter characterizing the steepness of this maximum. Let us note that the mean plate radius $\bar{a}$ is related to the value a_m by the following formula[22]:

$$\bar{a} = a_m(1 + 1/\mu)\,. \quad (2)$$

The particles have the complex refractive index $\tilde{n} = n + i\chi$.

Let the optical radiation be incident on the system of oriented plates oscillating about their steady state position. The integral formula for scattering coefficient into the back hemisphere, assuming the plates "strongly" oriented in space, is as follows:

$$\beta_{\pi_i} = \int N(a)\,\sigma_{\pi_i}\,da \quad (i = 1, 2, 3, 4), \quad (3)$$

where β_{π_i} are the scattering coefficients proportional to the corresponding parameters of the Stokes vector, $N(a)$ is the gamma-distribution function of the particle size defined by formula (1), σ_{π_i} ($i = 1, 2, 3, 4$) are the scattering cross sections.

The relationships for the scattering cross sections into the backward hemisphere were obtained in our paper[18] in the frameworks of the method of physical optics. The model presented makes it possible to calculate the light scattering characteristics at any point of the backward hemisphere for both polarized and unpolarized incident radiation at an arbitrary arrangement of the source, receiver, and particle. Thus, the formulas for the cross sections σ_{π_i} ($i = 1, 2, 3, 4$), obtained in Ref. 18 have the form

$$\sigma_{\pi_1} = W\left\{M_{11} + \frac{I_2}{I_1}M_{12} + \frac{I_3}{I_1}M_{13} + \frac{I_4}{I_1}M_{14}\right\},$$

$$\sigma_{\pi_2} = W\left\{M_{21} + \frac{I_2}{I_1}M_{22} + \frac{I_3}{I_1}M_{23} + \frac{I_4}{I_1}M_{24}\right\}, \quad (4)$$

$$\sigma_{\pi_3} = W\left\{M_{31} + \frac{I_2}{I_1}M_{32} + \frac{I_3}{I_1}M_{33} + \frac{I_4}{I_1}M_{34}\right\},$$

$$\sigma_{\pi_4} = W\left\{M_{41} + \frac{I_2}{I_1}M_{42} + \frac{I_3}{I_1}M_{43} + \frac{I_4}{I_1}M_{44}\right\}.$$

The factor W is determined by the wave number and the angular function, which is the Fraunhofer integral, I_i ($i = 1, 2, 3, 4$) are the Stokes vector parameters of the incident radiation, M_{ij} are the elements of the scattering phase matrix ($i = 1, 2, 3, 4$; $j = 1, 2, 3, 4$).

It is impossible to determine the values β_{π_i} from the corresponding lidar equations without attracting additional data, but their ratios

$$P_i = \frac{I_{\pi_i}}{I_{\pi_1}} = \frac{\beta_{\pi_i}}{\beta_{\pi_1}}, \; i = 2, 3, 4, \qquad (5)$$

can be measured directly in the experiment; I_{π_i} are the Stokes vector parameters of the scattered radiation. At laser sounding of disperse media one usually use a receiver capable of transforming the linearly polarized radiation or the radiation with circular polarization. So, in order to analyze the polarization properties of the scattered radiation, let us consider in this paper the values P_2 and P_4, respectively, for the cases of linear and circular polarization of the incident radiation.

Radiation becomes partially polarized at interaction of an unpolarized radiation with a crystal. The calculated results on the quantity defined by the formula

$$St = (I_{\pi_2}^2 + I_{\pi_3}^2 + I_{\pi_4}^2)^{1/2} / I_{\pi_1} \qquad (6)$$

allow one to study the dependence of the degree of polarization on different parameters of the particle.

Crystals under natural conditions oscillate about to their steady state position. Let us determine the scattering coefficient of an ensemble of ice plates taking into account their possible flatter, proportional to the intensity of the specular reflected radiation. Let us present the flatter angle by the pair of values (ψ', ξ), where ψ' (elevation angle) and ξ (azimuth angle) determine actual deviations of the direction normal to the plate from the axis O_3z_3 (Fig. 4).

Let the two-dimension random value (ψ', ξ) be uniformly distributed over the solid angle limited by the cone surface where $\xi \in [0, 2\pi]$, $\psi' \in [0, \psi]$. The calculations show that the change of the amplitude of the reflected signal at possible oscillations of the plates is mainly determined by the value ψ. Besides, one can ascertain this fact if analyzing the relevant azimuth dependences presented in our papers.[23,24] In order to decrease the calculation time by some orders of magnitude (without loss of the accuracy of calculations), it is sufficient to average over only the elevation angle ψ'. To do this, it is necessary to integrate the function $\beta_{\pi_i}(x)$ over the interval $[-\psi; \psi]$. As a result, we obtain

$$\beta_F(\psi) = \frac{1}{2\psi}\int_{-\psi}^{\psi}\beta_{\pi_1}(x)\,dx. \qquad (7)$$

Thus, formula (7) defines the scattering coefficient for the specular reflected radiation for the case of ice plates, which have a flatter.

Deviation of the receiving direction from the line of "strong" specular reflection leads to the displacement of the interval of integration by the same value. As a result, the coefficient $\beta_F(\psi,\vartheta)$ is determined by means of averaging the function $\beta_{\pi_i}(x)$ over the interval $[-\psi + \vartheta; \psi + \vartheta]$, i.e.,

$$\beta_F(\psi,\vartheta) = \frac{1}{2\psi}\int_{-\psi+\vartheta}^{\psi+\vartheta}\beta_{\pi_1}(x)\,dx. \qquad (8)$$

Discussion of the numerical calculations of the light scattering characteristics of plates

For qualitative analysis of the radiation reflected from the oriented plates with plane sides researchers use such a parameter as reflectivity. It is known that the reflectivity of ice for the incidence angles $0 \le \beta \le 60°$ is less that 10%, and for the angles $60 \le \beta \le 90°$ it sharply increases to almost 100%. To calculate the energy characteristics in the wave zone, the zone of the particle shadow along the direction perpendicular to the propagation of radiation is taken into account.

To obtain the quantitative estimates of light scattering characteristics, let us use the formulas for scattering coefficients (3). These relationships relate the polarization and energy properties of the reflected radiation to the physical characteristics of a polydisperse medium (size spectrum of semi-transparent particles), as well as to the wavelength and the state of polarization of incident radiation for a certain arrangement of the source, the receiver, and the plane of preferred orientation of the plates.

The values of the scattering coefficient β_{π_1} proportional to the intensity of the specular reflected radiation are shown in Fig. 5 for some realistic parameters of the particle size distribution $\bar{a}$, N, μ in a natural crystal cloud.

The "anomalously" high values of the scattering coefficient explain the fact that the photodetector was disabled in the majority of events when recording the specular reflection.[16,17] One can visually observe bright columns in the atmosphere, formed at reflection of light from plane sides of the oriented crystals. It is seen in Fig. 5 that as $\bar{a}$ increases by tens of microns, the amplitude of the specular reflected signal increases by several orders of magnitude.

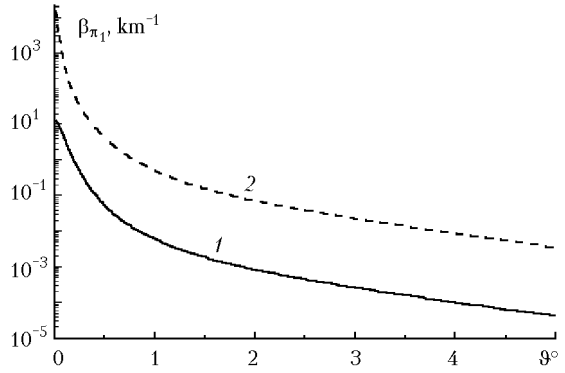

Fig. 5. Calculated values of the specular reflected coefficient β_{π_1} as a function of the displacement angle ϑ for the system of oriented plates at circular polarization of the incident wave. $\lambda = 0.694$ μm, $\tilde{n} = 1.31 + i\cdot10^{-3}$, $\mu = 5$, $\vartheta_1 = -40°$, $\vartheta_2 = 100°$, $\varphi_i = 0°$ ($i = 1, 2, 3$). $\overline{a} = 38$ μm, $N = 0.8$ l^{-1} (*1*); $\overline{a} = 100$ μm, $N = 25$ l^{-1} (*2*).

The values of the cross section proportional to the first parameter of the Stokes vector were presented in our earlier paper.[24] It was shown that, although there is the regular dependence of the cross section σ_{π_1} on the particle orientation in space with respect to the source and the receiver, the number of the extreme points on the curve σ_{π_1} is determined by a combination of the angles (φ_1, θ_1), (φ_2, θ_2), (φ_3, θ_3).

Theoretical investigation of the effect of anomalous backscattering as applied to the monostatic laser sounding was performed in Ref. 21. The values of the coefficient of specular reflection are presented there for the same parameters of the medium N, $\overline{a}$, μ that were used in calculating the values presented in Fig. 5. For example, at $\beta = 0°$, $\overline{a} = 37$ μm, $N = 0.8$ l^{-1}, $\mu = 5$ the value $\beta_{\pi_1} = 16.2$ km^{-1}. The backscattering coefficient measured in the experiment at the same parameters was equal to 17 km^{-1} (Ref. 17).

It is easy to ascertain by comparing numerical and experimental values that there is not only qualitative but also quantitative coincidence of these data. The value of the coefficient of specular reflection at $\beta = 20°$ and $\vartheta = 0°$ at corresponding parameters of the medium is equal to 11.6 km^{-1} (Fig. 5, curve *1*, the value β_{π_1} at $\vartheta = 0°$). In this case the higher value of $\beta_{\pi_1} = 16.2$ km^{-1} (at $\beta = 0°$) than $\beta_{\pi_1} = 11.6$ km^{-1} (at $\vartheta = 0°$ and $\beta = 20°$) is explained by the fact that, although the reflectivity at this angle is almost the same (differs by some per cent), the cross section of the specular reflected beam decreases as β increases.

The characteristic sign of the case of specular reflection is the sharp decrease of the amplitude of the recorded signal in scanning by the receiver from the direction corresponding to the "strong specular reflection." It follows from the analysis of data shown in Fig. 5 that even insignificant increase of ϑ leads to a noticeable change in the scattering coefficient β_{π_1}. The deviation of the receiver axis from the direction of specular reflection at bistatic sounding of the cloud containing oriented plates at the wavelength of $\lambda = 0.694$ μm by 1° leads to the decrease of the amplitude of the recorded signal by several orders of magnitude. One should note that the steepness of the characteristics β_{π_1} in the near-forward range ϑ is unambiguously related to the mean plate size $\overline{a}$ of the plate-shaped crystals. Let us note that such changes of scattering occur at any angle of radiation incidence on the plate.

The dependences of the ratios $\beta_{\pi_1}(\vartheta)/\beta_{\pi_1}(0)$ on the angle ϑ at different parameters $\overline{a}$ and μ are presented in Fig. 6 for the ensemble of "strongly" oriented ice plates (i.e., $\psi = 0°$). The areas between the curves *1* and *2*; *3* and *4*; *5* and *6*; *7* and *8* are continuously filled by the curves of $\beta_{\pi_1}(\vartheta)/\beta_{\pi_1}(0)$ displaced relative each other as obtained at different parameters μ from the interval [1, 10]. The curve with lower steepness corresponds to a larger μ value.

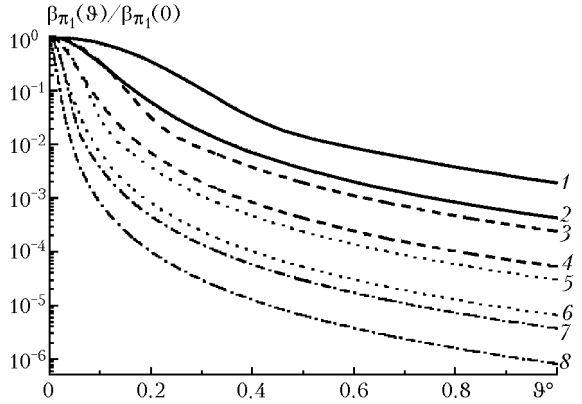

Fig. 6. The dependence of the scattering coefficient ratio $\beta_{\pi_1}(\vartheta)/\beta_{\pi_1}(0)$ for the system of strongly oriented plates. $\theta_1 = -40°$, $\varphi_1 = 0°$, $\theta_2 = 100°$, $\varphi_2 = 0°$, $\beta = 20°$, $\lambda = 0.694$ μm, $\tilde{n} = 1.31 + i\cdot10^{-3}$; $\overline{a} = 25$ μm, $\mu = 1$ (*1*), $\overline{a} = 25$ μm, $\mu = 10$ (*2*), $\overline{a} = 50$ μm, $\mu = 1$ (*3*), $\overline{a} = 50$ μm, $\mu = 10$ (*4*), $\overline{a} = 100$ μm, $\mu = 1$ (*5*), $\overline{a} = 100$ μm, $\mu = 10$ (*6*); $\overline{a} = 200$ μm, $\mu = 1$ (*7*), $\overline{a} = 200$ μm, $\mu = 10$ (*8*).

Such regularities were presented in Ref. 12 for the case of monostatic laser sounding. As numerical calculations showed, the relative characteristics $\beta_{\pi_1}(\vartheta)/\beta_{\pi_1}(0)$ and $\beta_F(\psi,\vartheta)/\beta_F(\psi,0)$ do not change at variations of β, but depend mainly on μ and $\overline{a}$.

As the parameter μ decreases, the quantity of plates of the radius greater than the mean one decreases.

Comparing two corresponding curves in Fig. 6 belonging to different areas, it is seen that the plates with a smaller base provide for lower steepness of the characteristic $\beta_{\pi_1}(\vartheta)/\beta_{\pi_1}(0)$. Besides, at the near-forward angles ϑ the rate of the change of the curve $\beta_{\pi_1}(\vartheta)/\beta_{\pi_1}(0)$ is mainly determined by the mean radii $\overline{a}$ of plates and, to a lower degree, by the parameter

μ. In the case of a bistatic sounding at a specular reflection angle in the near forward scanning with the lidar (or the optical receiver), one can judge about the mean plate radius from the change of the reflected radiation even if the distribution parameter μ is unknown. However, the accuracy of determining the value $\bar{a}$ significantly increases if the parameter μ has taken the values from the range less than [1; 10].

The directivity of the reflection from a system of ice plates with flatter also remains high, although it decreases as the angle ψ increases. Scattering is practically isotropic within the interval of 2ψ. The intensity of scattered field sharply decreases when crossing the boundaries of this range. Curves *2–6* in Fig. 7 correspond to this mechanism.

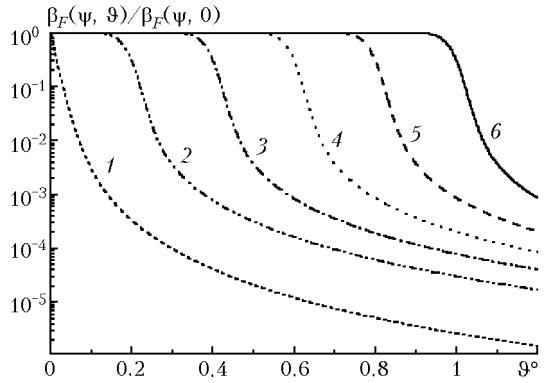

Fig. 7. The ratio of the specular reflected radiation scattering coefficient of the system of large plates ($\bar{a}$ = 200 μm) with flatter as a function of the displacement angle ϑ: $\varphi_1 = 0°$, $\theta_1 = -40°$, $\varphi_2 = 0°$, $\theta_2 = 100°$, $\beta = 20°$, $\lambda = 0.694$ μm, $N = 1\ 1^{-1}$, $\mu = 5$, $\tilde{n} = 1.31 + i\cdot 10^{-3}$; $\psi = 0$ (*1*), $\psi = 0.2°$ (*2*); $\psi = 0.4°$ (*3*); $\psi = 0.6°$ (*4*); $\psi = 0.8°$ (*5*); $\psi = 1°$ (*6*).

The length of the horizontal part, within which the scattering is isotropic, is determined for each dependence $\beta_F(\psi,\vartheta)/\beta_F(\psi,0)$ by the flatter angle ψ. The flatter angle for a relatively large mean plate size (Fig. 7) corresponds to the twofold decrease of the intensity of the reflected signal at near forward scanning by the receiver (or transmitter). However, such correspondence is broken for relatively large plates and small flatter.[26] Let us note that the steepness of the decreasing part practically does not depend on the flatter value, but is determined by the mean plate size. It should be noted that such a peculiarity of scattering is observed at any β angle, i.e., in the case of specular reflection at monostatic and bistatic sounding.

The information content of the polarization characteristics obtained at monostatic polarization laser sounding was studied in our earlier papers.[22] The peculiarities of the polarization characteristics caused by more complicated angular dependences are presented in Refs. 23, 24, 26 for the case when a transmitter and a receiver are spaced. Nevertheless, there are regular dependences of these values which exclude ambiguity in determination of the particle orientation at one or another state of polarization of the incident radiation. Let us present in this paper only some numerical calculations of the polarization parameters similar to those in Ref. 22, but for the case of bistatic sounding.

Let us note that orientation of the polarization plane of incident radiation with respect to the scatterer is unambiguously related with the azimuth angle φ_1.[18,24] Polarization characteristics $P_2(\varphi_1)$ at three different positions of particles with respect to the direction of the incidence of radiation in the case of linear polarization of the incident radiation are shown in Fig. 8.

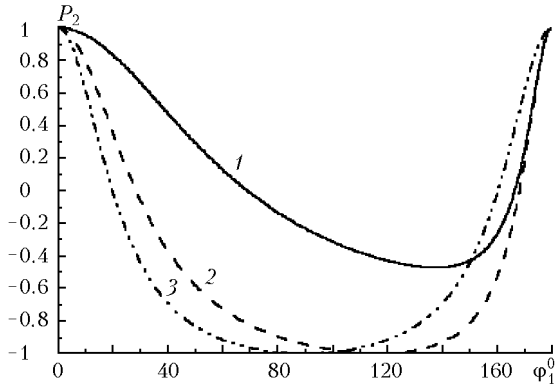

Fig. 8. The dependence $P_2(\varphi_1)$ at linear polarization of the incident radiation. $\lambda = 10.6$ μm, $\tilde{n} = 1.31 + i\cdot 10^{-4}$, $\varphi_2 = 0°$, $\theta_2 = 100°$; $\theta_1 = -40°$, $\beta = 20°$ (*1*), $\theta_1 = -10°$, $\beta = 35°$ (*2*), $\theta_1 = 0°$, $\beta = 40°$ (*3*).

It is seen in Fig. 8 that the position of minimum in each curve depends on the direction of sounding.

The values of the degree of polarization *St* calculated by formula (6) for different positions of particles for unpolarized incident radiation are shown in Fig. 9. Curves illustrating the change of the degree of polarization depending on the azimuth angle φ_1 have more steep slopes at large θ_1 angles.

It is seen from Fig. 9 that unpolarized radiation becomes almost completely linearly polarized after reflection from the plate at the change of φ_1 from 120 to 180°.

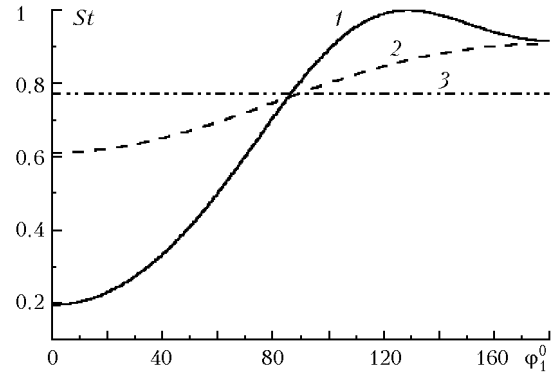

Fig. 9. The dependence of the degree of polarization *St* for the unpolarized incident radiation, $\lambda = 10.6$ μm, $\tilde{n} = 1.31 + i\cdot 10^{-4}$, $\varphi_2 = 0°$, $\theta_2 = 100°$; $\theta_1 = -40°$ (*1*); $-10°$ (*2*); $0°$ (*3*).

The refractive index of cloud crystals under natural conditions can differ from that of ice. In this connection, let us numerically investigate the dependences of the characteristics of reflected radiation on optical properties of the plates.

Figures 10 and 11 illustrate the change of the scattering cross section ratio $P_2 = \sigma_{\pi_2}/\sigma_{\pi_1}$ and $P_4 = \sigma_{\pi_4}/\sigma_{\pi_1}$ for linear and circular polarization of the incident radiation, respectively, as a function of the azimuth angle φ_1 for different refractive indices of the plate.

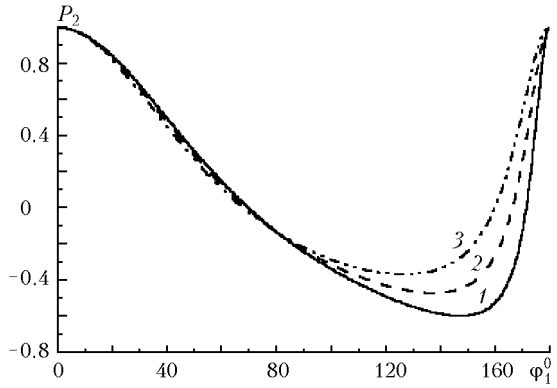

Fig. 10. The dependence $P_2(\varphi_1)$ at the linear polarization of the incident radiation. $\lambda = 10.6$ μm, $\tilde{n} = n + i\cdot 10^{-4}$, $\varphi_2 = 0°$, $\theta_2 = 100°$, $\theta_1 = -40°$; $n = 1.42$ (*1*), 1.31 (*2*); 1.21 (*3*).

The ratio P_2 is equal to unity in the case when the vector $\mathbf{E}_1$ of linearly polarized incident wave (in this case $\mathbf{E}_2 = 0$) lies in the incidence plane ($\varphi_1 = 0°$ or $\varphi_1 = 180°$). Each curve $P_2(\varphi_1)$ is not symmetric in the range from 0 to 180°. One or another position of the minimum of the curve $P_2(\varphi_1)$ corresponds to certain orientation of the incidence plane of electromagnetic wave and certain value of the refractive index of the particle. The polarization characteristic $P_4(\varphi_1)$ in the case of circular polarization of the incident radiation (Fig. 11) varies most strongly at φ_1 varying from 80 to 180°. The largest difference in the values P_4 for different refractive indices is observed at φ_1 close to 180°. Let us note that the possible flatter of plates (which is a few degrees[19]) does not lead to the noticeable change of the polarization characteristics.[26]

The dependences of the polarization characteristics in the case of unpolarized radiation incident at angle of approximately 20° for different $\tilde{n}$ values are shown in Fig. 12.

It is seen from Fig. 12 that the largest differences in the values St for different refractive indices are observed at $\varphi_1 = 180°$. Let us note that the change of the degree of polarization St is unambiguously related to variations of the angle β and the refractive index.

Thus, the polarization parameters have similar dependences on orientation and the refractive index of plates in the case of both bistatic and monostatic sounding. In this connection the obtained procedure of solving the inverse problem on determination of orientation and refractive index from the data of polarization characteristics of monostatic sounding can be also used in the case of bistatic sounding.[21]

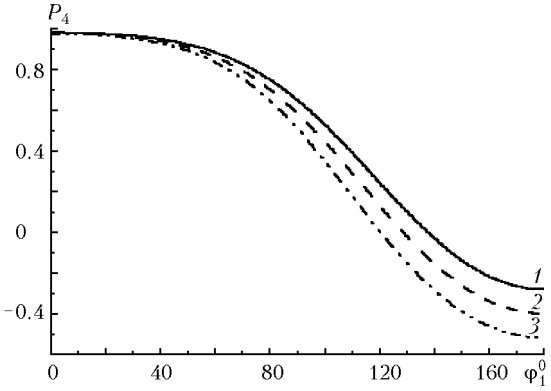

Fig. 11. The dependence $P_4(\varphi_1)$ at the circular polarization of the incident radiation. $\lambda = 10.6$ μm, $\tilde{n} = n + i\cdot 10^{-4}$, $\varphi_2 = 0°$, $\theta_2 = 100°$, $\theta_1 = -40°$, $n = 1.42$ (*1*); 1.31 (*2*); 1.21 (*3*).

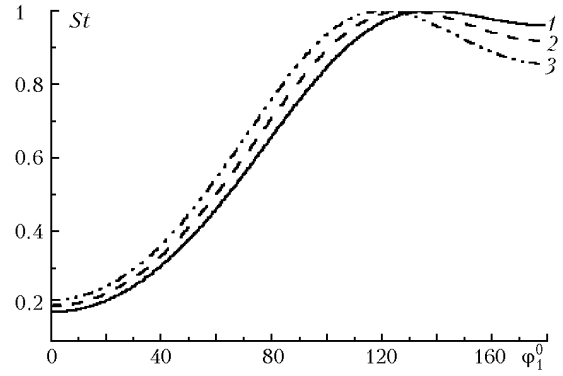

Fig. 12. The dependence $St(\varphi_1)$ for the unpolarized incident radiation. $\lambda = 10.6$ μm, $\tilde{n} = n + i\cdot 10^{-3}$, $\varphi_2 = 0°$, $\theta_2 = 100°$, $\theta_1 = -40°$, $n = 1.42$ (*1*); 1.31 (*2*); 1.21 (*3*).

Conclusion

Ice plates are among the water ice crystals comprising ice clouds, and, as a rule, their fraction is higher than that of other crystals of other habits. In the case of stable orientation of extended particles the intensity of specular reflection from plates taking into account their possible oscillations significantly (by several orders of magnitude) exceeds the corresponding characteristic of any other oriented crystals. Hence, the model of cloud in the form of an ensemble of oriented plates taking into account their flatter presented in this paper can be used for solving the direct and inverse problems on inverting the data of monostatic and bistatic sounding of crystal clouds. The advantages of the lidar system, when the source and the receiver are spaced lie in the fact that the high-amplitude polarized signal bearing information on optical, orientation, and microphysical properties of the volume under investigation can be obtained at sounding of the ice atmospheric formation of a complex structure.

Analysis of numerical calculations of the light scattering characteristics has revealed that the flatter of plates and parameters of the particle size distribution can be determined from the data on the relative characteristics of the specular reflected radiation obtained at near forward scanning with the lidar. The refractive index and the position of plates relative to the source and the receiver can be determined from the data on the polarization characteristics of reflected signal, which practically do not depend on the small angle of flatter and the particle size distribution.

Acknowledgments

The work was supported in part by Russian Foundation for Basic Research (Grant No. 01–05–65209), Ministry of Industry and Science (Grant "High-altitude polarization lidar" No. 06–21).

References

1. O.A. Volkovitskii, L.N. Pavlova, and A.G. Petrushin, *Optical Properties of Crystal Clouds* (Gidrometeoizdat, Leningrad, 1984), 200 pp.
2. A. Mallman, J.L. Hock, and R.G. Greenler, Appl. Opt. **37**, 1441–1449 (1998).
3. K. Sassen and W. Arnott, Appl. Opt. **37**, 1420–1426 (1998).
4. W.A. Cooper and G. Vali, J. Atmos. Sci. **38**, 1244–1259 (1981).
5. A.G. Petrushin, in: *Problems of Atmospheric Physics* (Gidrometeoizdat, Leningrad, 1998), pp. 118–150.
6. H.-R. Cho, J.V. Iribarne, and W.G. Richards, J. Atmos. Sci. **38**, 1111–1114 (1981).
7. M.V. Kabanov, *Regional Monitoring of the Atmosphere.* Part 1. *Scientific-Methodical Principles* (SB RAS, Tomsk, 1997), 211 pp.
8. B.A. Tinsley and G.W. Deen, J. Geophys. Res. D **96**, No. 12, 22283–22295 (1991).
9. T.C. Marshall, W.D. Rust, W.P. Winn, K.E. Gilbert, J. Geophys. Res. D **20**, No. 2, 2171–2181 (1989).
10. K. Sassen, J. Optics & Photonics News, No. 3, 39–42 (1999).
11. B.M. Welsh and C.S. Gardner, Appl. Opt. **28**. No. 1, 32–82 (1989).
12. A.A. Popov, "*Development and investigation of calculation methods for some classes of applied problems of electrodynamics.*" Doct. Dissert. Phys.-Math. Sci., Ioshkar-Ola (1992), 400 pp.
13. M.I. Mischenko, J.W. Hovenier, and L.D. Travis, eds., *Light Scattering by Nonspherical Particles. Theory, Measurements, and Application* (Academic Press, International standard book number: 0-12-498660-9, California, USA, 2000), 690 pp.
14. D.N. Romashov, Atmos. Oceanic Opt. **12**, No. 12, 1025–1028 (1999).
15. A.A. Popov, Proc. SPIE **2822**, 186–194 (1996).
16. C.M.R. Platt, J. Appl. Meteorol. **17**, No. 4, 482–488 (1978).
17. C.M.R. Platt, N.L. Abshire, and G.T. McNice, J. Appl. Meteorol. **17**. No. 8, 1220–1224 (1978).
18. O.V. Shefer, Atmos. Oceanic Opt. **12**, No. 7, 549–553 (1999).
19. J. Hallett, J. Opt. Soc. Am. A. **4**, No. 3, 581–589 (1987).
20. A. Heymsfield, J. Atmos. Sci. **34**, 367–381 (1977).
21. A.A. Popov and O.V. Shefer, J. Appl. Opt. **33**, No. 30, 7038–7044 (1994).
22. A.A. Popov and O.V. Shefer, J. Appl. Opt. **34**, No. 4, 1488–1492 (1995).
23. O.V. Shefer, Atmos. Oceanic Opt. **15**, No. 10, 804–809 (2002).
24. O.V. Shefer, Atmos. Oceanic Opt. **14**, No. 8, 607–612 (2001).
25. K. Sassen, J. Opt. Soc. Am. **4**, No. 3, 570–580 (1987).
26. O.V. Shefer, Atmos. Oceanic Opt. **16**, No. 4, 318–324 (2003).